Hindawi Publishing Corporation
Journal of Ceramics
Volume 2015, Article ID 298690, 7 pages
http://dx.doi.org/10.1155/2015/298690

Research Article

Cubic Phases in the Gd_2O_3-ZrO_2 and Dy_2O_3-TiO_2 Systems for Nuclear Industry Applications

Maria Teresa Malachevsky,[1,2] Diego Rodríguez Salvador,[1] Sergio Leiva,[1] and Claudio Alberto D'Ovidio[1]

[1]*Centro Atómico Bariloche, CNEA, Avenida Bustillo 9500, 8400 San Carlos de Bariloche, Argentina*
[2]*CONICET, Argentina*

Correspondence should be addressed to Maria Teresa Malachevsky; malache@cab.cnea.gov.ar

Received 22 June 2015; Accepted 27 July 2015

Academic Editor: Jim Low

Neutron absorbers are elements with a high neutron capture cross section that are employed at nuclear reactors to control excess fuel reactivity. If these absorbers are converted into materials of relatively low absorption cross section as the result of neutron absorption, they consume during the reactor core life and so are called burnable. These elements can be distributed inside an oxide ceramic that is stable under irradiation and thus called inert. Cubic zirconium oxide is one of the preferred materials to be used as inert matrix. It is stable under irradiation, experiments very low swelling, and is isomorphic to uranium oxide. The cubic phase is stabilized by adding small amounts of dopants like Dy_2O_3 and Gd_2O_3. As both dysprosium and gadolinium have a high neutron cross section, they are good candidates to prepare burnable neutron absorbers. Pyrochlores, like $Gd_2Zr_2O_7$ and $Dy_2Ti_2O_7$, allow the solid solution of a large quantity of elements besides being stable under irradiation. These characteristics make them also useful for safe storage of nuclear wastes. We present a preliminary study of the thermal analysis of different compositions in the systems Gd_2O_3-ZrO_2 and Dy_2O_3-TiO_2, investigating the feasibility to obtain oxide ceramics useful for the nuclear industry.

1. Introduction

At the beginning of a reactor cycle, the fuel presents an excess reactivity to compensate future fuel depletion and fission products buildup. This is controlled by using burnable neutron absorbers or neutron poisons, that is, by inclusion into the fuel assembly materials with a large neutron cross section. If the absorbers are incorporated directly into the fuel, they are called continuous or homogeneous [1, 2]. When the burnable neutron absorbers are dispersed into an inert matrix, they are called discrete or inhomogeneous and they are distributed among the fuel pellets. As these can be prepared independently of the fuel and with no limitations in their handling and storage, we focused on their preparation.

Zirconium oxide is a good candidate to be used as inert matrix mainly because of its stability under irradiation and its compatibility with reactor materials [3]. It accommodates both fission materials and neutron absorbers. Actually, CANDU reactor has among the 43 bars that compose the fuel element a central bar that includes a neutron absorber in zirconium oxide inert matrix [4].

Zirconium oxide has three polymorphic phases: it is monoclinic up to 1443 K, tetragonal up to 2643 K, and cubic up to its fusion at 2953 K. It is impossible to prepare a single-phase material with a particular crystalline structure due to these phase transformations that proceed during cooling. Thus the cubic phase is stabilized by adding small amounts of dopants (about 8 mol%) like Y_2O_3, CaO, or MgO [5]. There is an added interest in the cubic phase as it is isomorphic to uranium oxide, even if any of the polymorphs can be employed as inert matrix. The stabilized zirconia is not amorphized under irradiation and its swelling under fast neutron is neglectable, as happens with the fluorite structure [6, 7].

Due to their chemical resemblance with Y_2O_3, Gd_2O_3 stabilizes the cubic phase of the zirconium oxide. As this oxide has a large cross section for neutron capture, it is a good candidate to prepare burnable poisons in zirconia inert matrix [8].

Table 1: Selected compositions for the mixtures.

ID	wt%				Characteristic
	Gd_2O_3	Dy_2O_3	ZrO_2	TiO_2	
GdZr1	33.31	—	66.69	—	Eutectoid
GdZr2	59.62	—	40.38	—	Pyrochlore
GdZr3	76.30	—	23.70	—	Eutectoid
GdZr4	87.86	—	11.14	—	Eutectic
GdZr5	94.00	—	6.00	—	Eutectoid
DyTi1	—	82.34	—	17.66	Polymorph
DyTi2	—	76.07	—	23.93	Eutectic
DyTi3	—	70.01	—	29.99	Pyrochlore
DyTi4	—	49.65	—	50.35	Eutectic

Pyrochlores are oxides of the form $A_2B_2O_7$, with a structure that is closely related to the fluorite structure [9]. Its phase stability is basically determined by the A and B cationic radius ratio, as similar cationic radii are more likely to form as disordered fluorites than ordered pyrochlores. Pyrochlores are excellent host matrices for nuclear waste immobilization because they can dissolve various lanthanides, actinides, and other elements which are generated inside nuclear reactors [10–14]. It has been found that stability of the pyrochlores under irradiation increases with the decrease in radius ratio. There is another related phase of interest, dysprosium titanate Dy_2TiO_5, that is an effective burnable poison that has been successfully employed for several years as control rod in Russian reactors [15].

In the present work, we focus on the feasibility to obtain cubic phases that could be employed as burnable neutron absorbers, studying composition and suitable sintering temperatures. We also investigate the feasibility of forming a cubic pyrochlore phase and titanates. Two different systems are investigated: Gd_2O_3-$ZrO_2$and Dy_2O_3-TiO_2.

2. Materials and Methods

We started with Gd_2O_3 and Dy_2O_3 99.9% from Alfa Aesar and ZrO_2 and TiO_2 99.9% from Sigma Aldrich. Appropriate amounts of each oxide were mixed in an attrition mill at 200 rpm for 30 minutes with 2 mm yttria stabilized zirconia balls. We prepared the mixtures in stoichiometries corresponding to particular compositions of interest identified in the corresponding binary phase diagram. The selected compositions are presented in Table 1.

We prepared 20 g of each mixture, adding an organic binder so as to reproduce the conditions needed for preparing a pellet. For the compositions in the system Gd_2O_3-ZrO_2, a mixture of 1.5 wt% sodium alginate and 3 wt% methylcellulose was employed. For the Dy_2O_3-TiO_2 systems, 5 wt% of polyvinyl butyral (PVB) was employed as binder.

We carried out simultaneous thermal analysis (STA) in a Netzsch 449 F1 Jupiter to determine sintering conditions and phase formation. Measurements were performed inside a SiC furnace with maximum working temperature of 1828 K, at a rate of 5 K/min in helium atmosphere. The balance resolution was of 0.025 μg and the temperature was measured with a resolution of 1 μW. After the analysis, the existent phases were identified by X-ray diffraction using the program HighScore Plus version 3.0.4.

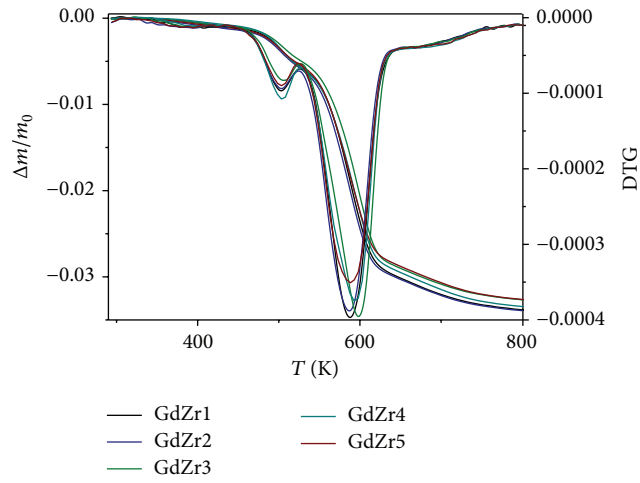

Figure 1: TG/DTG from room temperature to 800 K.

Based on these results, we selected three compositions to verify the formation of the desired phases after sintering: GdZr1, GdZr2, and DyTi4. Pellets were prepared by uniaxial pressing at 1000 atm. These were sintered in air with a slow heating rate of 1 K/min up to 773 K to eliminate the binder, followed by a faster heat-up at 2 K/min to the sintering temperature (1973 K for GdZr1, 1873 K for GdZr2, and 1673 K for DyTi4). After a dwell time of 2 hours, the pellets were cooled in the furnace.

3. Results and Discussion

3.1. Gd_2O_3-ZrO_2 System. In Figure 1, we present the mass evolution with temperature TG and its derivative DTG, from room temperature to 800 K. There is a first weight loss starting at about 450 K coincident with the binder decomposition, followed by a marked weight loss that starts at about 530 K and ends at 800 K with the complete elimination of this additive. This behavior is similar for all the samples measured as the binder and its proportion are the same in all of them.

From 800 K up to 1270 K there is a slight mass loss, as can be observed in Figure 2, that can be related to carbon elimination from the binder and/or impurities present in the starting oxides. From 1270 K to the final temperature, about 1 mg of mass is lost. Sample GdZr4 shows an additional mass loss at about 1200 K.

In Figure 3 we present the DTA results. From the phase diagram, several solid-solid phase transformations can be associated with the observed peaks. Pyrochlore transforms to fluorite at 1800 K, there is a eutectoid transformation to fluorite at 1400 K, zirconium oxide transforms from monoclinic to tetragonal at 1500 K, and gadolinium oxide transforms from cubic to monoclinic at 700 K.

For sample GdZr1 a small endothermic peak is detected at 321 K that can be associated with the eutectic transformation

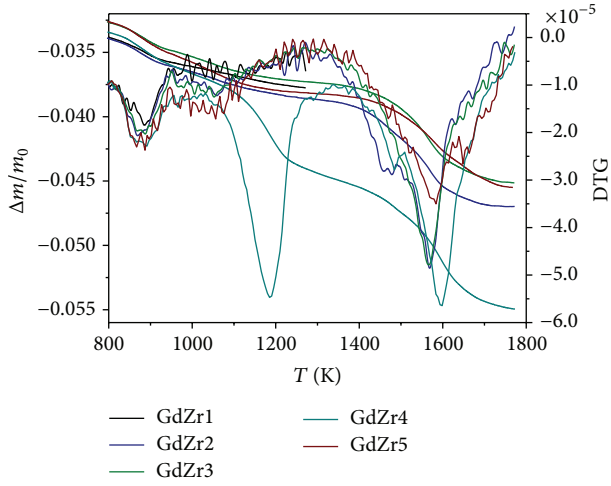

Figure 2: TG/DTG from 800 K to the end of the test.

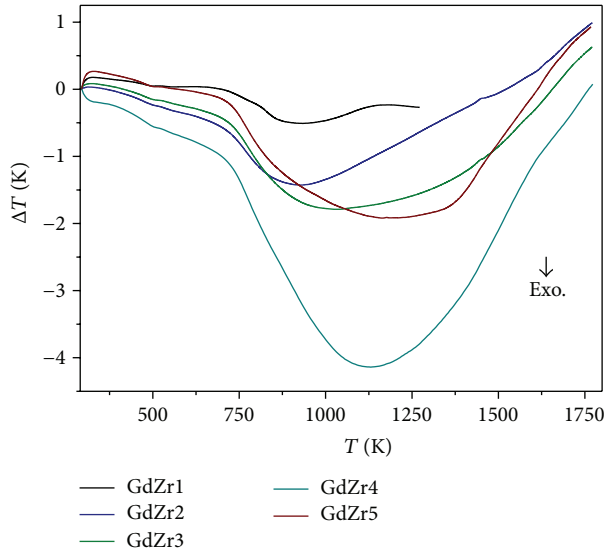

Figure 3: DTA as a function of temperature.

to the cubic phase. This temperature is lower than the 400 K reported in the phase diagrams. An X-ray analysis of the powders at the end of the test showed the presence of monoclinic ZrO_2 and cubic Gd_2O_3.

The pyrochlore phase present in sample GdZr2 transforms to fluorite at 1800 K. Both phases were detected by X-ray diffraction at the end of the test. The eutectoid transformation to fluorite of sample GdZr3 takes place at 1400 K and ZrO_2 (present in both GdZr2 and GdZr3) transforms to a tetragonal phase around 1500 K. All these solid-solid transformations are represented at the beginning of the endothermic peaks observed in the studied temperature range. These peaks are consequent to the mass loss observed in the TG measurement from 1270 K. This loss is not detected in sample GdZr1 as the intensity of the endothermic peak is lower. X-ray diffraction confirms the existence of tetragonal ZrO_2 in samples GdZr2 and GdZr3.

A wide exothermic peak is observed in all samples, starting at 700 K that can be originated by a phase transformation from cubic to monoclinic in the gadolinium oxide, coincident with X-ray diffraction phase detection. The behavior of samples GdZr4 and GdZr3 is similar, as expected from the system's phase diagram. In both samples this peak is wider, being better defined in sample GdZr4.

In Figure 4 we present the X-ray diffraction patterns obtained on the powders after the STA measurement. The major phases are indicated, but other minor phases were identified. These are fluorite in GdZr1, tetragonal ZrO_2 and fluorite in GdZr2, GdZr4, and GdZr5, and tetragonal ZrO_2 and pyrochlore in GdZr3.

3.2. Dy_2O_3-TiO_2 System. In Figure 5, the mass loss with temperature can be followed. The loss up to 800 K corresponds to the binder decomposition and elimination.

In Figure 6 we show the DTA measurements. The phases detected by X-ray diffraction after the STA test is completed are those expected from the phase diagram. We present the identified phases for samples DyTi2 and DyTi4 in Figure 7. Initially, a small endothermic peak is observed in all samples associated with the binder decomposition and loss. A wide peak is observed around 600 K. At this fast heating rate, the formation of new phases as dysprosium titanate and pyrochlore is not complete and this peak includes the transformation of TiO_2 from anatase to rutile. The endothermic peak starting at 1600 K observed in samples DyTi1 and DyTi2 corresponds to polymorphic changes of the Dy_2TiO_5 towards cubic structures. The same peak observed in samples DyTi3 and DyTi4 can be associated with the $Dy_2Ti_2O_7$ pyrochlore transforming to the hexagonal structure Dy_2TiO_5.

3.3. Sintered Pellets. Pellets were polished and observed with the scanning electron microscope (SEM). Both samples GdZr1 and GdZr2 are similar and presented a large quantity of pores, as can be observed in Figures 8(a) and 8(b). DyTi4 is quite dense and two different phases homogeneously distributed along the sample can be easily identified (Figure 8(c)). As confirmed by EDS, the darker phase is TiO_2 and the lighter phase corresponds to the pyrochlore $Dy_2Ti_2O_7$, being an excellent candidate for use as burnable poison.

In order to determine the phase formation in the samples of the Gd_2O_3-ZrO_2 system, X-ray diffraction of the pellets was performed. In GdZr1 the major phase identified is cubic ZrO_2, showing that gadolinium oxide effectively stabilized the zirconia even if the transition could not be identified by the STA measurement in this sample. $Gd_2Zr_2O_7$ pyrochlore and cubic Gd_2O_3 are also present in lower quantities. In GdZr2 the major phases are $Gd_2Zr_2O_7$ pyrochlore and tetragonal ZrO_2. Other ZrO_2 polymorphs are also present in low quantities. Even if zirconia is not in the fluorite structure, this material could be employed as burnable poison.

4. Conclusions

Pyrochlores phase stability is basically determined by the A and B cationic radius ratio, as similar cationic radii are

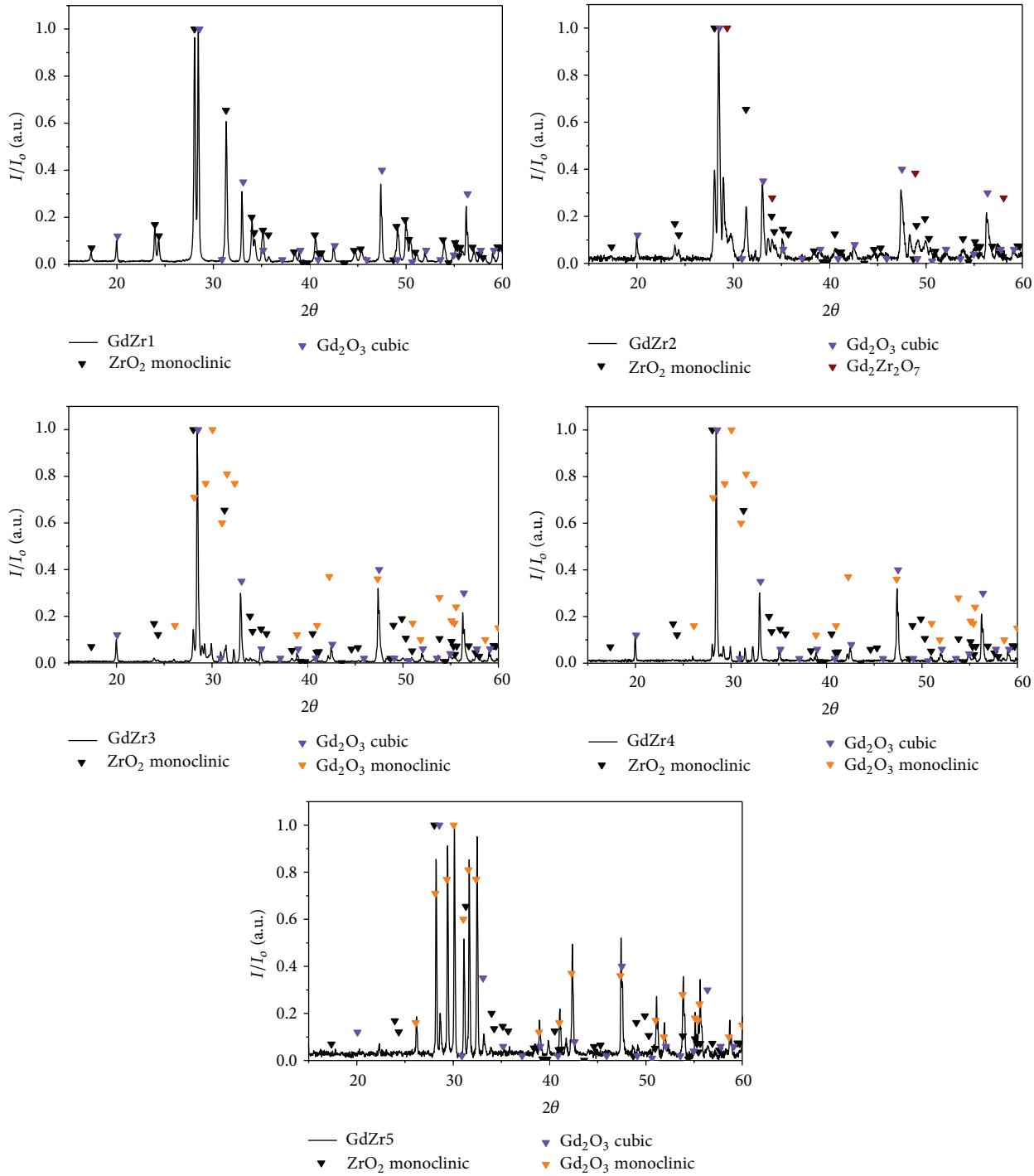

Figure 4: X-ray diffraction of the samples after the STA measurement.

more likely to form as disordered fluorites than ordered pyrochlores. Taking into account that $r_{Dy}/r_{Ti} \approx 1.412$ and $r_{Gd}/r_{Zr} \approx 1.253$, a pyrochlore phase should be more easily achieved in the Dy_2O_3-TiO_2 system. We were able to acknowledge that the Gd_2O_3-ZrO_2 system needs higher temperatures than the Dy_2O_3-TiO_2 system to form cubic phases. Excluding sample GdZr1, for all the studied compositions the eutectoid transformation to fluorite was detected. This indicates a relative ease for cubic phase formation independent of the amount of gadolinium oxide employed, making this system suitable for developing burnable poisons in inert matrix.

For the Dy_2O_3-TiO_2 system, X-ray diffraction reveals that dysprosium titanate Dy_2TiO_5 is in its hexagonal phase but the cubic $Dy_2Ti_2O_7$ pyrochlore can be easily synthesized at low temperatures.

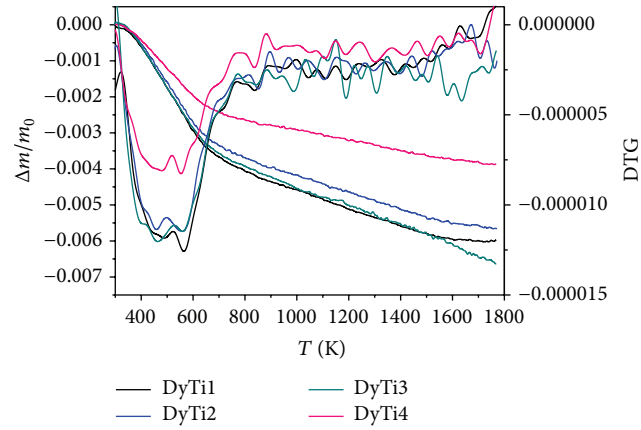

Figure 5: TG-DTG as a function of temperature.

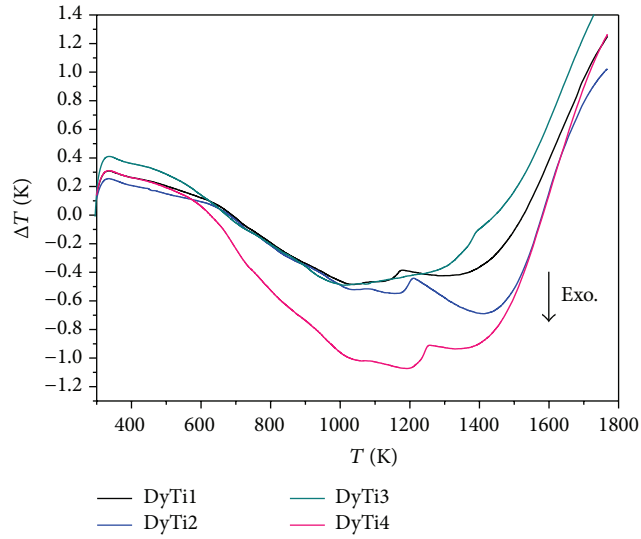

Figure 6: DTA as a function of temperature.

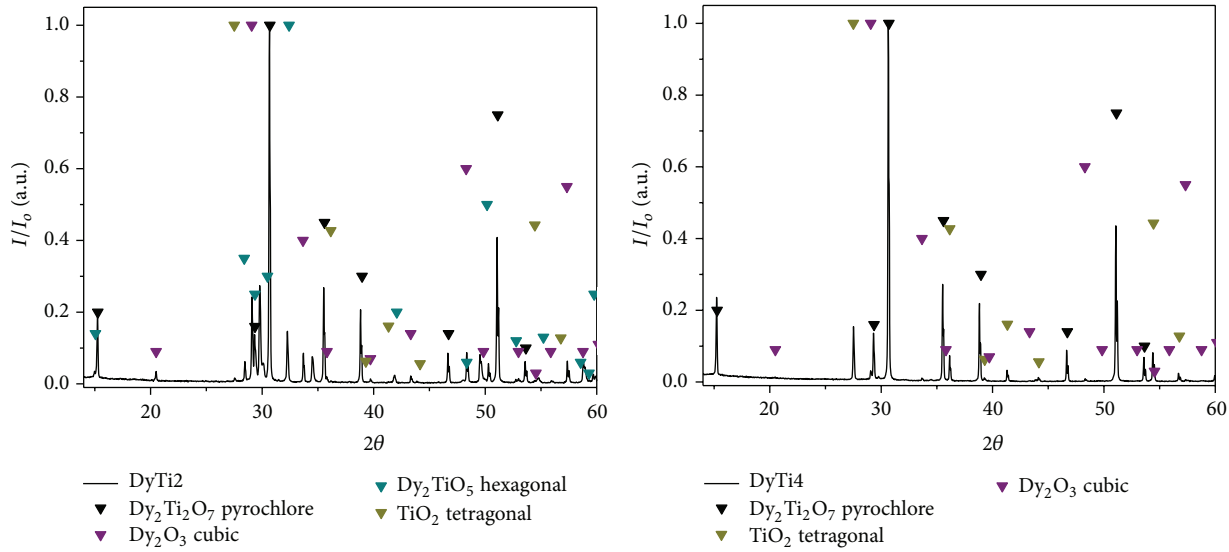

Figure 7: X-ray diffraction of the samples after the STA measurement.

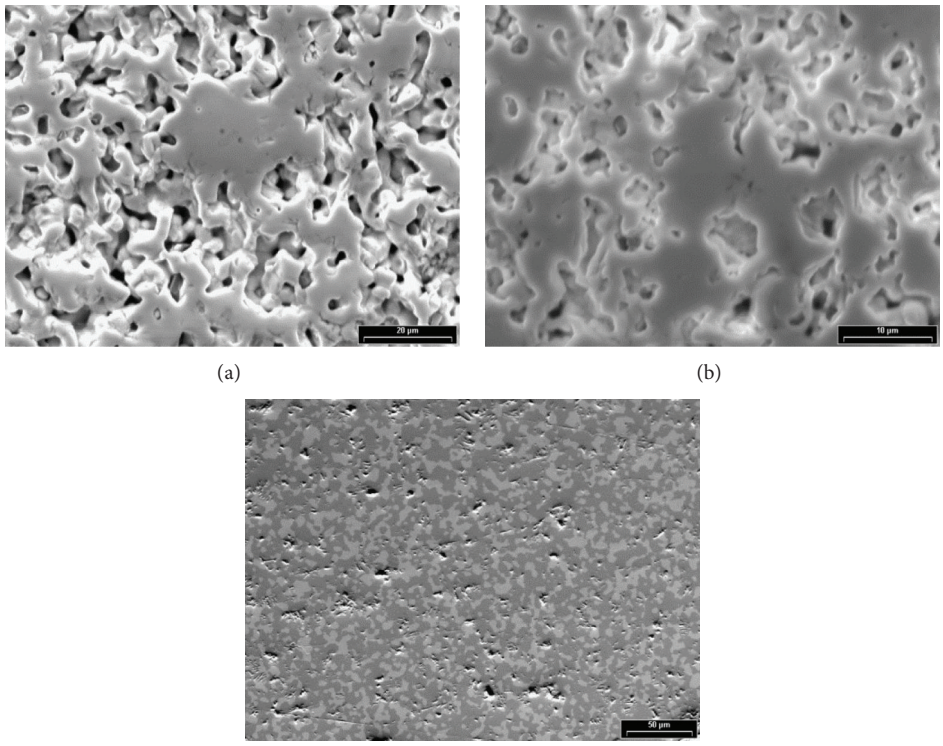

(a) (b)

(c)

Figure 8: SEM photographs of the polished surface of the sintered pellets: (a) GdZr1, (b) GdZr2, and (c) DyTi4.

Some pellets were sintered to verify the STA measurement observations. The cubic zirconia phase was effectively stabilized in sample GdZr1, even if the fluorite transformation could not be identified in the STA measurement. Pyrochlores were successfully sintered in both GdZr2 and DyTi4 samples.

Both systems present adequate conditions to fabricate an oxide ceramic material for nuclear applications.

Conflict of Interests

The authors declare that there is no conflict of interests regarding the publication of this paper.

References

[1] T. Cardinaels, J. Hertog, B. Vos, L. de Tollenaere, C. Delafoy, and M. Verwerft, "Dopant solubility and lattice contraction in gadolinia and gadolinia–chromia doped UO_2 fuels," *Journal of Nuclear Materials*, vol. 424, no. 1–3, pp. 289–300, 2012.

[2] T. Jevremovic, *Nuclear Principles in Engineering*, Springer, 2nd edition, 2009.

[3] G. Velişa, A. Debelle, L. Thomé et al., "Implantation of high concentration noble gases in cubic zirconia and silicon carbide: a contrasted radiation tolerance," *Journal of Nuclear Materials*, vol. 451, no. 1–3, pp. 14–23, 2014.

[4] AECL, "ACR-1000 technical description," AECL Report 10820-01372-230-002, Atomic Energy of Canada, 2010, Revision.

[5] M. Yoshimura, *Ceramic Bulletin*, vol. 34, pp. 1950–1955, 1988.

[6] G. Ledergerber, C. Degueldre, P. Heimgartner, M. A. Pouchon, and U. Kasemeyer, "Inert matrix fuel for the utilisation of plutonium," *Progress in Nuclear Energy*, vol. 38, no. 3-4, pp. 301–308, 2001.

[7] W. J. Carmack, M. Todosow, M. K. Meyer, and K. O. Pasamehmetoglu, "Inert matrix fuel neutronic, thermal-hydraulic, and transient behavior in a light water reactor," *Journal of Nuclear Materials*, vol. 352, no. 1–3, pp. 276–284, 2006.

[8] H. S. Kim, C. Y. Joung, B. H. Lee, S. H. Kim, and D. S. Sohn, "Characteristics of $Gd_xM_yO_z$ (M = Ti, Zr or Al) as a burnable absorber," *Journal of Nuclear Materials*, vol. 372, no. 2-3, pp. 340–349, 2008.

[9] B. P. Mandal, M. Pandey, and A. K. Tyagi, "$Gd_2Zr_2O_7$ pyrochlore: potential host matrix for some constituents of thoria based reactor's waste," *Journal of Nuclear Materials*, vol. 406, no. 2, pp. 238–243, 2010.

[10] M. Lang, F. Zhang, J. Zhang et al., "Review of $A_2B_2O_7$ pyrochlore response to irradiation and pressure," *Nuclear Instruments and Methods in Physics Research B: Beam Interactions with Materials and Atoms*, vol. 268, no. 19, pp. 2951–2959, 2010.

[11] B. P. Mandal, N. Garg, S. M. Sharma, and A. K. Tyagi, "Solubility of ThO_2 in $Gd_2Zr_2O_7$ pyrochlore: XRD, SEM and Raman spectroscopic studies," *Journal of Nuclear Materials*, vol. 392, no. 1, pp. 95–99, 2009.

[12] M. Jafar, P. Sengupta, S. N. Achary, and A. K. Tyagi, "Phase evolution and microstructural studies in $CaZrTi_2O_7$ (zirconolite)–$Sm_2Ti_2O_7$ (pyrochlore) system," *Journal of the European Ceramic Society*, vol. 34, no. 16, pp. 4373–4381, 2014.

[13] E. J. Harvey, K. R. Whittle, G. R. Lumpkin, R. I. Smith, and S. A. T. Redfern, "Solid solubilities of $(La\ Nd,)_2(Zr,Ti)_2O_7$

phases deduced by neutron diffraction," *Journal of Solid State Chemistry*, vol. 178, no. 3, pp. 800–810, 2005.

[14] B. P. Mandal, R. Shukla, S. N. Achary, and A. K. Tyagi, "Crucial role of the reaction conditions in isolating several metastable phases in a Gd-Ce-Zr-O system," *Inorganic Chemistry*, vol. 49, no. 22, pp. 10415–10421, 2010.

[15] V. D. Risovany, E. E. Varlashova, and D. N. Suslov, "Dysprosium titanate as an absorber material for control rods," *Journal of Nuclear Materials*, vol. 281, no. 1, pp. 84–89, 2000.